We are uploading our point-by-point response to all referee comments and specify all changes in the revised manuscript, combined with a marked-up manuscript version showing the changes.

Response to Reviewer 1:

We are very grateful to your comments for the manuscript. They have important guiding significance for our manuscript and our research work. We have revised the manuscript according to your comments. The response to each revision is listed as follows:

Comment 1:

The method of detection of anomalies of the borehole strain, is not well-known to non-specialists, and – I would say – to the specialists neither. In my opinion, at least one additional explanatory paragraph entirely devoted to this subject is needed, in the "Introduction" Section.

Response:

This is a constructive suggestion! We did not mention the background of negentropy in the "Introduction" Section. An explanatory paragraph has been supplemented. The corresponding references are also added to the "References" Section.

Changes:

We have supplemented an explanatory paragraph in the "Introduction" Section:

"Hence, it is implied that possible precursor anomalies lead to an increase in disordered components of observation data during earthquake preparation processes. K. Eftaxias et al. (2008) proved that the pre-catastrophic stage could break the persistency and high organization of the electromagetic field through studying fractional-Brownian-motion-type model using laboratory and field experimental electromagetic data. In view of Lévy flight and Gaussian processes, Lévy flight mechanism prevents the organization of the critical state to be completed, since the long scales are cut-off due to the Gaussian mechanism (S.M. Potirakis et al., 2019).

Entropy can serve as a measure of the unknown external energy flow into the seismic system (Akopian, S. T., 2014). K. Karamanos et al (2005, 2006) quantified and visualized temporal changes of the complexity by approximate entropy, they claimed significant complexity decrease and accession at the tail of the preseismic electromagetic emission could be diagnostic tools for the impending earthquake. Yukio Ohsawa (2018) detected earthquake activation precursors by studying the regional seismic information entropy on earthquake catalog. Angelo De Santis (2011) recalled the Gutenberg - Richter law and considered the negative logarithm of b-value is the entropy of the magnitude frequency of earthquake occurrence associated with two earthquakes in Italy.

Negentropy definition is based on the entropy and it is also widely used to detect non-Gaussian features. Yue Li (2018) proposed an arrival-time picking method based

on negentropy for microseismic data. In this study, the negentropy is applied to borehole strain at Guza station associated with the Wenchuan earthquake, approximated by skewness and kurtosis. Subsequently we study the extracted negentropy anomalies in different scales to investigate correlations with crustal deformation."

Comment 2:

In my opinion, in Fig. 6, "kurtosis=0.28699skewnessˆ2-0.28696" should boil down to "kurtosis=0.287(skewnessˆ2-1)", I mean that in equation (9), A=B which is a Remarkable result, if it holds true !!! At least one additional explanatory paragraph entirely devoted to this result is needed, in the "Discussion and Conclusions" Section !

Response:

We can change the parabolic relation into "kurtosis=0.287(skewnessˆ2-1)". Since in our case, A is always equal to -B because the kurtosis and skewness of the study period were normalized. There are

$$E(skewness) = E(kurtosis) = 0, \tag{1}$$

and

$$D(kurtosis) = E(kurtosis^2) = D(skewness) = E(skewness^2) = 1. \tag{2}$$

According to equation (9) in the manuscript and equation (1) and (2), there is

$$\begin{aligned} E(kurtosis) &= E(A \cdot skewness^2 + B) = \frac{1}{n}\sum_{i=1}^{n}(A \cdot skewness^2(i) + n \cdot B) \\ &= A \cdot \frac{1}{n}\sum_{i}^{n} skewness^2(i) + B \\ &= A \cdot D(skewness) + B \\ &= A + B = 0 \end{aligned} \tag{3}$$

Thanks to your inspiration, we have derived a new relation based on this relation and supplemented it after equation (9) in the "Methodology" Section. Besides, the corresponding explanation has been supplemented in "Discussion and Conclusions" Section.

Changes:

We have supplemented an addition equation after equation (9) in Line 101-103 in the "Methodology" Section:

"Here we calculate the normalized skewness and kurtosis in the study period, so equation (9) can be derived into

$$kurtosis(X) = A \cdot (skewness^2(X) - 1), \tag{10}$$

indicating when the negentropy is outside the range (-1,1), the test day is super-Gaussian."

We have also supplemented an explanatory paragraph. But combined with the comments of reviewer 2, the explanatory paragraph was not shown in the final revised

manuscript.

"In the skewness-kurtosis domain, we observed the evolution of the negentropy distribution prior to the earthquake. Negentropy gradually transformed its distribution to a parabolic relation since July 2007, indicating a relatively stable state was broken due to the non-Gaussian mechanism ."

Comment 3:

In line 153, is stated that "k*=1.1130". What is the meaning of keeping so many significant digits ? Why not " k*=1.1 " or "k*=1.11" ? Please explain ! At least one additional explanatory paragraph is needed !

Response:

The meaning of k* value itself is a threshold for extracting negentropy anomalies. First, k* is calculated by Otsu's method by searching for k when the within-class variance of negentropy becomes the maximum, according to equations (10) to (13). Second, the format of the negentropy depends on the sample data. The YRY-4 borehole strainmeter has a measurement accuracy of 10^{-9}, but in practical calculations, we usually cutoff four digits after the decimal point. Therefore, the calculated k* is consistent with the accuracy of the negentropy and the strain data, resulting in 5 significant digits.

In fact, when we take the threshold k* as 1.1 or 1.11, there are 367 or 363 anomaly days respectively in study period (912 days), which is almost no difference with "k*=1.1130" (363 anomaly days). However, we still keep this result for the above reason when the numbers of anomalies are counted and accumulated.

Changes:

We have supplemented an explanatory paragraph after Line 131:

"Otsu threshold k* here is consistent with the accuracy of the negentropy and the strain data, The YRY-4 borehole strainmeter has a measurement accuracy of 10^{-9}, however, we usually cutoff four digits after the decimal point in practical calculations."

Comment 4:

In line 157, Fig.5, explain the Units !

Response:

X-axis and y-axis of the Fig. 5 are negentropy and its variance. The negentropy is defined as the weighted square of skewness and kurtosis in equation (6) in this manuscript. Because the skewness and kurtosis can be seen as ratios according to equation (7) and (8), there are no units.

Minor corrections:

(1) - In line 17, “earthqake” → “earthquake” !
It has been modified.

(2) - In lines 26 and 27, the citation has no uniform style !
(M.J.S. Johnston et al., 2006, Chi S. L. et al., 2014) has been modified as (Johnston M.J.S. et al., 2006, Chi S. L. et al., 2014).

(3) - In lines 295 and 296, of the References list, there are quotation marks in the title of the Reference. This is the only place in the whole list where this happens !
It has been modified.

(4) - In line 153, there are superscripts in the middle of the sentence, for no reason !
It has been modified.

(5) - In line 157, the end dot (final punctuation mark) is missing !
It has been added.

(6) - In line 159, it is mentioned “Fig 6(a)” instead of the correct “Fig. 6(a)” (the dot is missing) !
It has been added.

(7) - In line 297, “Gutenber” → “Gutenberg” !
It has been modified.

(8) - In line 325, the style is not uniform ! Dots are missing !
It has been modified.

References:

K. Karamanos, A. Peratzakis, P. Kapiris, S. Nikolopoulos, J. Kopanas and K. Eftaxias. Extracting preseismic electromagnetic signatures in terms of symbolic dynamics. Nonlinear Processes in Geophysics 12, 835-848, 2005.

K. Karamanos, D. Dakopoulos, K. Aloupis, A. Peratzakis, L. Athanasopoulou, S. Nikolopoulos, P. Kapiris and K. Eftaxias. Study of pre-seismic electromagnetic signals in terms of complexity. Phys. Rev.E 74, 016104 – 016125, 2006.

K. Eftaxias, Y. Contoyiannis, G. Balasis, K. Karamanos, J. Kopanas, G. Antonopoulos, G. Koulouras and C. Nomicos. Evidence of fractional-Brownian-motion-type asperity model for earthquake generation in candidate pre-seismic electromagnetic emissions. Nat. Haz. Earth Syst. Sci. 8, 657-669, 2008.

S. M. Potirakis, Y. Contoyiannis and K. Eftaxias. Levy and Gauss statistics in the preparation of an earthquake. Physica A, Vol. 528, 15 August 2019, 121360 (In Press)

De Santis, A., et al.: The Gutenberg-Richter Law and Entropy of Earthquakes: Two Case Studies in Central Italy. Bulletin of the Seismological Society of America 101(3): 1386-1395, 2011.

Li, Y., et al.: Arrival-time picking method based on approximate negentropy for microseismic data. Journal of Applied Geophysics 152: 100-109, 2018.

Ohsawa, Y.: Regional Seismic Information Entropy to Detect Earthquake Activation Precursors. Entropy 20(11), 2018.

Akopian, S. T.: Open dissipative seismic systems and ensembles of strong earthquakes: energy balance and entropy funnels. Geophysical Journal International 201(3):

1618-1641, 2015.

Response to Reviewer 2:

We are very grateful to your comments for the manuscript. They have important guiding significance for our manuscript and our research work. We have revised the manuscript according to your comments. The response to each revision is listed as follows:

1. The manuscript is mostly well organized and written, the figures are mostly of sufficient quality excepted Fig.1 which is too dark and lack details about the active faults and the earthquake rupture location.

Response:

Thank you for your suggestion. Fig.1 in the manuscript is not professional enough. We have updated the figure with the active faults and the earthquake rupture location. Besides, we have supplemented three stations aiming to discuss our findings in the "Confusion discussion" Section.

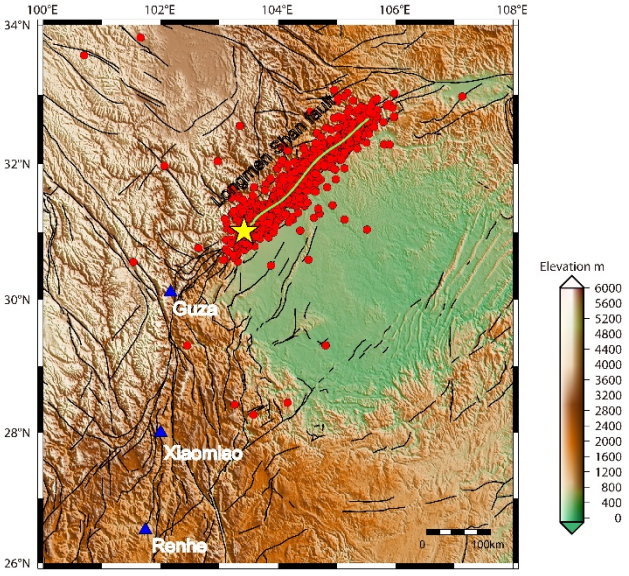

Fig. 1 Location map showing the epicentre of the Wenchuan earthquake and three stations. The epicentre was located in Wenchuan County, Sichuan Province, at 31.01°N, 103.42°E. The red circles are aftershocks (Ms>3.0) from the main shock to October 2008. The green curve is the schematic curve of the main rupture zone and the black curves are faults.

2. Major comment 1:

- *In particular, the nearest strain station (GUZA) is located far from the earthquake source (150 km), so that the network configuration to study strain precursors is far to*

be optimal. If the precursory phase implied widespread crustal changes, some changes should have been detected by other sensors, therefore other set of data (GPS? Seismometers? Groundwater? ...) located in the near-field of the earthquake should be analyzed. Despite strainmeters are highly sensitive instruments, I have concerns about their capability to detect subtle strain changes at such large distance. Strain signals are mostly sensitive to local variations (hydrology, rain, air pressure, ...), so it would be interesting to see precipitation, groundwater and barometric records near GUZA station if available. I agree that the observed strain changes are spurious and the fact that they may roughly coincide with the onset time of the event makes them even more interesting, but there is absolutely no evidence that they are linked to the precursory phase of the earthquake. If the negentropy increased before the earthquake, why did it stay to a high level months after the rupture (Fig. 4)?
In particular at L. 305-307 (and also L. 296-299), the authors stated that Â´n negentropy anomalies ... may be a reflection of the subsurface medium and fault activities in the focal area associated with the Wenchuan earthquake Â¨z. This is a strong conclusion which came with no proof. Thus, based on only one station, the authors should point out that some strain changes are spurious but they shouldn't try to link these changes to the precursory phase with such a few observations. Therefore, the Discussion section should be modified and it should be clearly stated that further data are required to decipher a potential precursory phase.

Response:

Thank you very much for your suggestion.

We agree the "Discussion and Conclusion" section is kind of unreasonable based on the borehole strain data of one station.

Referring to your guiding suggestions above, we have studied the correlation between the negentropy anomalies and the Wenchuan earthquake through three parts. 1. Comparison of random time periods. 2. Comparison of different stations. 3. Exclusion of co-seismic events and weather factors.

We first introduce the three supplemented parts and answer your other specific questions next.

Changes:

We have divided the "Discussion and Conclusion" Section into "Confusion Discussion" Section and "Conclusion" Section.

We have also discussed our findings more carefully in the "Confusion Discussion" Section and objectively stated further researches are required to decipher a potential precursory phase in the "Conclusion" Section.

To study the correlation between extracted anomalies and earthquakes, Parrot (2011) proposed a method for random earthquake distribution. The location of the earthquake epicentre is randomly changed, but the size of the study area and the study time is kept unchanged. The anomalous variation is compared between the random region and the

actual seismic region, and the correction between the anomalies and the earthquake is determined. In order to verify the relationship between negentropy anomalies and the Wenchuan earthquake, we did a similar random earthquake distribution study as follows.

1. Comparison of random time periods.

We randomly selected March 20, 2011 and March 24, 2014 as the random earthquake days, and study the strain data for 200 days before and after the earthquake days at Guza station. The selected periods are required to be in the absence of strong earthquakes and with higher quality. We performed negentropy analysis on these two random periods and compared them with the results of negentropy analysis associate with the Wenchuan earthquake as shown in Fig. 2.

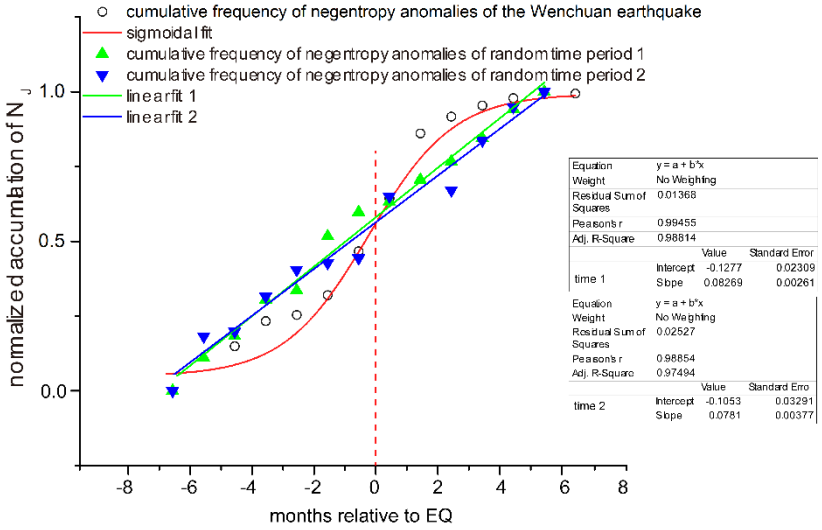

Fig. 2 The comparative analysis of cumulative frequency of negentropy anomalies between earthquake period and random time periods. The green triangles correspond to the random earthquake on March 20, 2011, the blue triangles correspond to the random earthquake on March 24, 2014.

As we can see in Fig. 2, the cumulative frequency of negentropy anomalies of random periods have statistical linear increases. However, in the Wenchuan earthquake periods, as the earthquake approaches, the cumulative frequency of negentropy anomalies increases rapidly and recovered to a slow growth after the earthquake.

2. Comparison of different stations.

We supplemented two other stations to find out if their observations received strain changes. We chose Xiaomiao station and Renhe station, their locations are shown in Fig. 1. Corresponding to the Guza station, we did the negentropy analysis of the two stations as shown in Fig. 3.

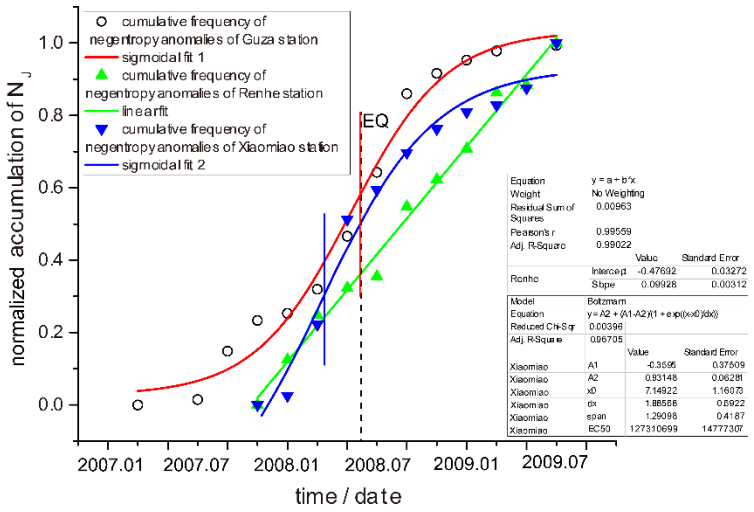

Fig. 3 Cumulative frequency of negentropy anomalies of Xiaomiao station and Renhe station from September 16, 2007 to June 30, 2009. The negentropy analysis of Guza station is from January 1, 2007 to June 30, 2009, because of the different installation time of the instruments. The red vertical line is the inflection point of the fitting curve of Guza station. The blue vertical line is the inflection point of the fitting curve of Xiaomiao station. The black dashed line is the earthquake day.

As we can see in the Fig. 3, the cumulative frequency of negentropy anomalies of Xiaomiao station are also well fitted by the sigmoid function. The accumulation curve is growing rapidly before the earthquake and concave downward after which is similar to the Guza station, although the inflection point of Xiaomiao station is about two months preceding the earthquake moment. However, since the curve is approximately linear before and after the inflection point, the value of inflection point exists a range.

Cumulative anomalies of the Renhe station are basically linear, indicating that the Renhe stations may don't receive pre-earthquake anomalies.

Renhe station is far from the end of the Wenchuan earthquake fault, according to the fracture mechanics, so it is reasonable that no abnormal changes are observed. However, Xiaomiao station is located between the Guza station and Renhe station, it may receive some changes. The fitting result also shows that there is a similar trend to the Guza station, with a weaker curvature. So, for the nearest station to the epicentre, Guza station may able to receive more pre-earthquake anomalies.

Furthermore, Qiu (2012) found that the anomalies at Ningshan station were similar to the anomalies at Guza station. Such two stations have observed similar Wenchuan earthquake precursor anomalies, which may not be accidental. Since the Ningshan station is actually located at the northeastern end of the Longmenshan fault zone. This location is a correspondence with the southwestern end of the fault where the Guza station is.

3. Exclusion of co-seismic events and weather factors.

We studied the Earthquake events data from the USGS National Earthquake Information Center (NEIC) catalog instead of continuous seismic waveforms recorded by seismometers, and consider all the Ms3.0+ events in the catalog which occurred in the study region during the study period as shown in Fig. 4(a). We count the multiple earthquakes occurred in one day as one event. Comparing the results in the manuscript,

we accumulate the earthquake event as Fig. 4(b). Before the earthquake, the cumulative frequency of earthquake events increased linearly, indicating there was no rapid growth phase of earthquake events in the region. This phenomenon is different from the cumulative frequency of negentropy anomalies extracted by borehole strain, which also verify that the co-seismic events didn't cause the pre-earthquake anomalies recorded by borehole strain before the Wenchuan earthquake at Guza station. While after the Wenchuan earthquake, there is a rapid growth rate of the cumulative frequency due to numerous aftershocks. With the restoration of the crust in the seismic source region, the accumulation after the Wenchuan earthquake is gradually slow, which is similar to the accumulation of negentropy anomalies after the earthquake at Guza station.

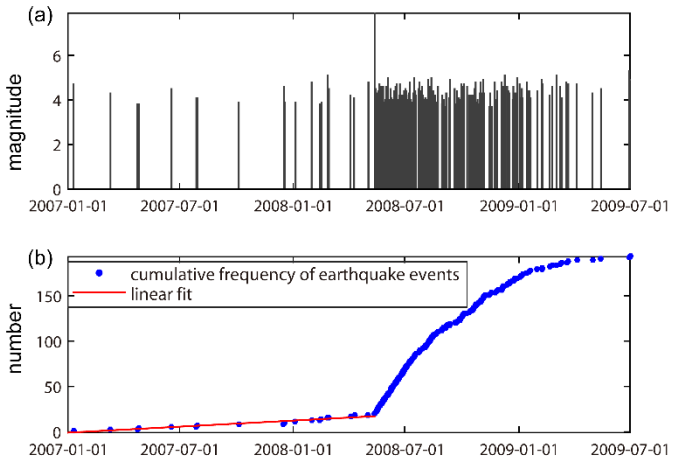

Fig. 4 Earthquake catalog (Ms>3.0) of the study region during the study period and the cumulative frequency of earthquake events.

We also agree that strain signals are mostly sensitive to a few meteorological factors, such as the air pressure, temperature and rainfall. The water level data of Guza station are not available before 2009. As shown in Fig. 5, we display the detrend borehole strain, pressure variations, temperature variations recorded at Guza station and the daily rainfall measured by Tropical Rainfall Measuring Mission (TRMM) satellite which are downloaded through the NASA GIOVANNI-4 for the same period and the same area (http://giovanni.gsfc.nasa.gov/giovanni/) . There are clearly annual variations in the strain, air pressure, temperature and rainfall data. The air pressure and temperature have been steadily fluctuating within a certain range, and the rainfall is also shown to be more in summer and less in winter.

While we calculated the differential data of the strain for negentropy analysis. So, we make differential calculations for all three influencing factors as shown in Fig. 6.

We observed that the air pressure, temperature and rainfall didn't change abnormally during the period when the extracted anomalies increase, whether we do differential calculation.

To further examine the correlation, we calculated the correlation coefficient in each sliding window (win=15 days) between the factors and the strain, and the results are shown in the Fig. 7. Although the original factors and the original strain are not strongly corrected, the correlation coefficients of differential data are far less than those of the

original data. Therefore, we consider that the abnormal variations on the processed strain signals are not caused by these factors.

Thanks for your suggestion, we revisited the strain for different time periods, different stations and factors, then discussed them carefully. Considering the structure of the manuscript, for the meteorological factors, we have only briefly discussed and excluded them. A revised manuscript was attached in the updated manuscript.

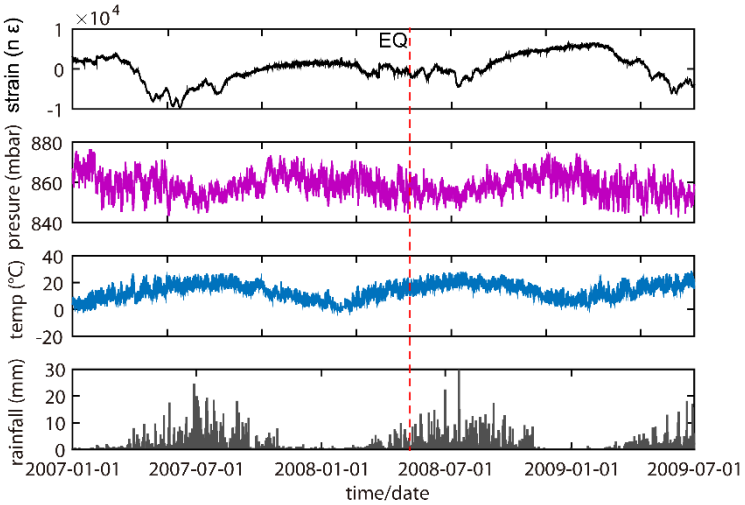

Fig. 5. Borehole stain, air pressure, temperature and rainfall variations during study period at Guza station

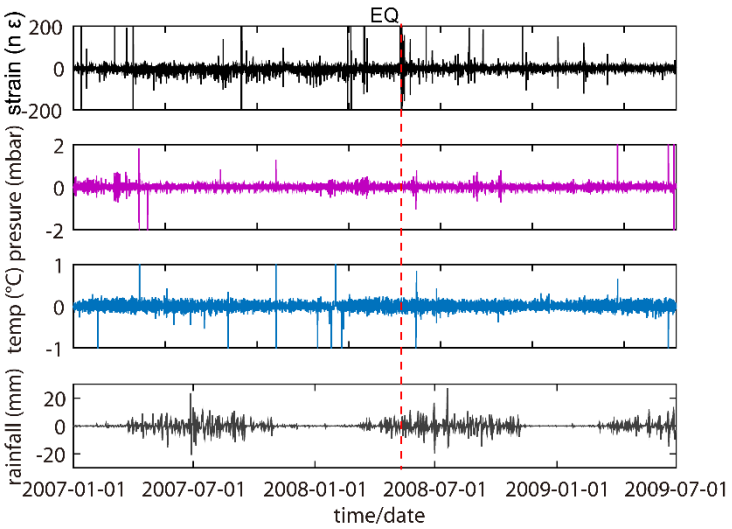

Fig. 6. Differential borehole stain, air pressure, temperature and rainfall variations during study period at Guza station

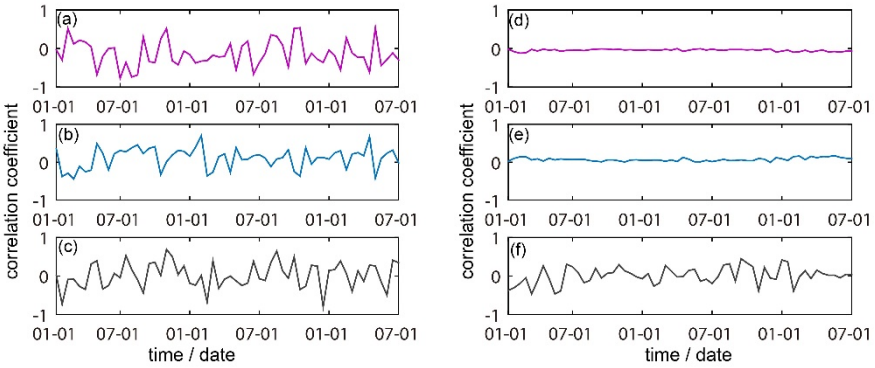

Fig. 7 (a), (b) and (c) are the results of correction coefficient between air pressure, temperature, rainfall and strain. (d), (e) and (f) are the results of correction coefficient between differential air pressure, differential temperature, differential rainfall and differential strain.

We detailed the method of data pre-processing in major comment 2.

*# **[1]** In particular, the nearest strain station (GUZA) is located far from the earthquake source (150 km), so that the network configuration to study strain precursors is far to be optimal.*

Response:

As for the earthquake-monitoring capability of the borehole strain, Su Kaizhi (1991) comprehensively considered the time characteristics of the strainmeters detection capability, the amplitude distribution of the strain precursor and the occurrence time of the strain precursor, started with the general relationship between the time scale and the detected minimum strain amplitude, the epicenter distance and the magnitude, and magnitude and the occurrence time of the strain precursors, combined with observations of Chinese borehole strainmeters, and therefore obtained the estimated monitoring and controlling extent of long- and medium-term, short-term, and impending precursors. For the long-term precursor phase of the earthquakes of Ms8.0, the borehole strainmeter has a monitoring capability radius of about 430 km, and for the short-term and impending precursors, the scope is more than 700 km. So, the Wenchuan earthquake source is within the monitoring capability of the borehole strainmeter at Guza station.

Besides, in the Fig. 1, we find the Guza station stands on the southwestern end of the Longmenshan fault zone. From the point of view of fracture mechanics, the end point of the fracture is where the stress concentrated or even the singularity occurs (Qiu Z. H., 2012). According to this view, we think that the strainmeter is possible to record information related to earthquakes at Guza Station.

Changes:

We have supplemented a short explanation for this distance in Line 56-58.

*# **[2]** If the precursory phase implied widespread crustal changes, some changes should have been detected by other sensors, therefore other set of data (GPS? Seis- mometers?*

Groundwater? ...) located in the near-field of the earthquake should be analyzed.

Response:

We agree that it would be better to analyze other sets of data such as GPS and seismometers which may record some changes. Unfortunately, some data are limited for us for now. However, we can provide a few explanations.

Firstly, because borehole strainmeters are designed to record deformation that lies between the spectral coverage of seismometers and GPS, and are ideal for capturing strain transients that occur in periods of hours to years as shown in Fig. 8, we choose borehole strain to study the pre-earthquake changes.

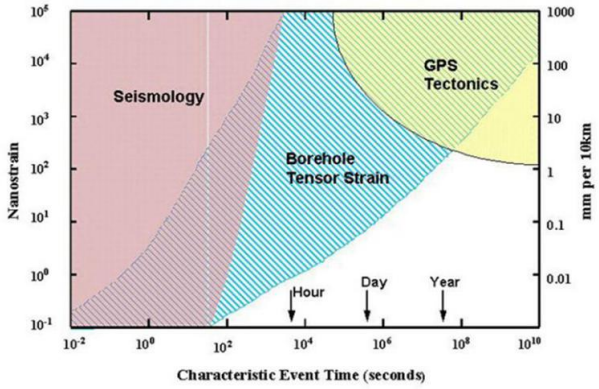

Fig. 8 shows Instrumental characteristics of seismology, borehole tensor strain and GPS tectonics. Source: http://www.earthscope.org. Borehole strain are ideal for revealing short-term (from seconds to years); Seismographs are mainly used to determine relevant seismic parameters; GPS is a relatively long-term observation (from weeks to decades).

Secondly, we studied the Earthquake events data from the USGS NEIC catalog instead of continuous seismic waveforms recorded by seismometers. The comparison result is in Fig. 4.

However, different instruments record signals of different characteristics. We are not sure about the possibility that the crustal changes are recorded by other sensors. Besides, we investigated the outgoing longwave radiation (Kong X., et al., 2018), radon concentrations in water (Yan R., et al., 2011), water level and water temperature data (Sun X. L., et al., 2016) before the earthquake. There are some similarities between their results and the results in our manuscript. (We quoted their results at the end of this response.)

Thirdly, according to the principle of the YRY-4 strainmeter, the four observations Si, ($i=1,2,3,4$) are sampled by four independent sensors. This means that the sensors in the four directions do not affect each other. We can think that the anomalies before and after the Wenchuan earthquake were recorded simultaneously by four sensors.

Changes:

We have stated the further data and further researches are needed to confirm a potential precursor phase in "Conclusion" Section.

*# **[3]** If the negentropy increased before the earthquake, why did it stay to a high level months after the rupture (Fig. 4)?*

Response:

This is the empirical phenomenon after the main shock in the hypocentral region. The Wenchuan earthquake is main-aftershock type. After the Wenchuan earthquake, the earth's crust was still in a very unstable stage. As of October 2008, more than 900 aftershocks (Ms>3.0) occurred as shown in the Fig. 1. Therefore, the negentropy stay to a high level after the rupture.

In addition, with the restoration of the crust in the seismic source region, the accumulation of negentropy anomalies after the earthquake is growing slower as shown in Fig. 8 in the manuscript.

 # [4] In particular at L. 305-307 (and also L. 296-299), the authors stated that Ân negentropy anomalies ... may be a reflection of the subsurface medium and fault activities in the focal area associated with the Wenchuan earthquake. This is a strong conclusion which came with no proof.

Response:

Thank you for your suggestion. This conclusion is indeed too positive. The mechanism for these abnormal changes is needed to be discussed further. What we want to express is the extracted negentropy anomalies may be related to the Wenchuan earthquake.

We have modified the conclusions more prudently in “Conclusion” Section.

Major comment 2:

It’s not clear which data the authors use for the statistical analysis. Equations (1) and (2) describe the protocol to derive areal strain from borehole gauge measurements and they show that the 3 ways provide roughly similar areal strain signal. However, in L. 91-92, the authors calculate the difference in the data. Why that? And what does this sentence (L. 91-92) means? Is it the difference in strain data which is used for negentropy analysis? If yes, why not using directly the areal strain signals which are a robust measure of crustal strain changes? The authors removed tidal strain, but what about borehole trend and air pressure correction? The description of the data is confusing and should be improved.

Response:

Thank you for your suggestion. We did not describe the data pre-processing part clearly, especially in L. 91-92. The detailed process is as follows.

First, equations (1) and (2) in the manuscript describe the protocol to derive areal strain from borehole strainmeters. Then we show the component data satisfy self-consistent through Fig. 2 in the manuscript to illustrate that the areal strain can replace the observations of four components.

Second, we processed the areal strain. The procedures and reasons of data pre-

processing are as follows.

Step 1: Differential calculation

We set the areal strain data as $X(n)$ and differential areal strain data as $Y(n)$, we know $Y(n)=X(n)-X(n-1)$, $F_X(e^{j\omega})$ is frequency characteristic of $X(n)$, $F_Y(e^{j\omega})$ is frequency characteristic of $Y(n)$ according to differential properties based on Fourier transform

$$F_Y(e^{j\omega})=(1-e^{-j\omega})F_X(e^{j\omega})$$

This process can be equivalent to a filtering system, let the frequency response of this system be $H_1(e^{j\omega})$, then

$$\left|H_1(e^{j\omega})\right|=\left|\frac{F_Y(e^{j\omega})}{F_X(e^{j\omega})}\right|=\left|1-e^{-j\omega}\right|$$
$$=\sqrt{2(1-\cos\omega)}$$

It can be seen that when ω is very small or 0, the frequency response is 0, indicating that the Step 1 removes the low frequency information of the signal, including borehole trend and low frequency effects of the air pressure and temperature on the signal.

Step 2: Harmonic analysis

We remove the periodic term that still exists through daily harmonic analysis. We set the fitting function as Fourier series. The reserved signal $Z(n)$ can be simplified as

$$Z(n)=Y(n)-\sum_{k=1}^{n}A_k\sin(k\omega_0 n+\varphi_i)$$

$F_Z(e^{j\omega})$ is frequency characteristic of $Z(n)$, this process can also be seen as a filtering system, let the frequency response of this system be $H_2(e^{j\omega})$.

$$\left|H_2(e^{j\omega})\right|=\left|\frac{F_Y(e^{j\omega})-\sum_k \pi A_k[\delta(\omega-k\omega_0)-\delta(\omega+k\omega_0)]/2}{F_Y(e^{j\omega})}\right|$$

Minimize $Z(n)$ by least squares method in time domain, then ideally for the system gain

$$\left|H_2(e^{j\omega})\right|=\begin{cases}0 & \omega=k\omega_0\\ 1 & \omega=others\end{cases}$$

The frequency response after two steps is

$$|H(e^{j\omega})| = |H_1(e^{j\omega})H_2(e^{j\omega})| = \begin{cases} 0 & \omega = k\omega_0 \\ \sqrt{2(1-\cos\omega)} & \omega = others \end{cases}$$

Therefore, the Step 2 removes the periodic terms in the signal. We think the period terms here mainly includes the periods related to the solid tide, also includes the periodic effects of air pressure.

Finally, we performed the negentropy analysis for the processed data.

We randomly selected one day to explain the effects of the data pre-processing as shown in Fig. 9.

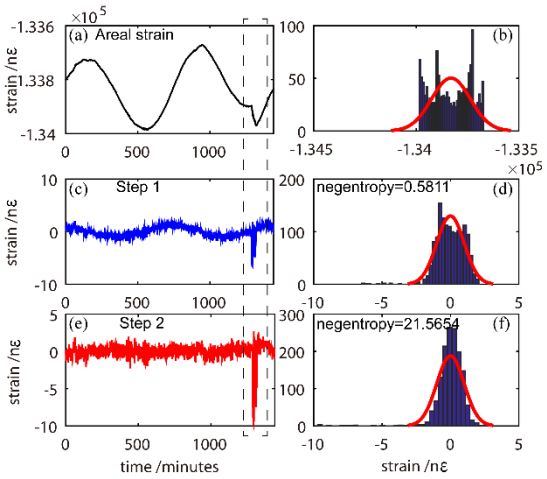

Fig. 9. (a). Areal strain of January 19, 2009. (c). Areal strain after differential calculation. (e). Differential areal strain after harmonic analysis. (b), (d), and (f) are the data distribution of (a), (c) and (c).

There is an abnormal change on the original areal strain curve at about 1400 minutes in Fig. 9(a). The areal strain is obviously non-Gaussian in Fig .9(b). The data presents a U-shaped distribution, and its negentropy has no meaning. This change becomes obvious after the differential calculation (Fig. 9(c)), but the negentropy is small due to the amplitudes of the periodic terms (Fig. 9(d)). After the harmonic analysis, the negentropy value increases significantly (Fig. 9(f)). Therefore, the small changes in the curve are amplified by the data pre-processing.

Our ultimate goal is to study negentropy (non-Gaussian characteristic) of the signals. The low frequency components and periodic components affect the Gaussian characteristic of the areal strain signals. This is why we processed the areal strain signals, although the areal strain is a robust measure of crustal strain changes. We are more concerned about the remaining high frequency variations. This is what we want to express in L. 91-92 in the manuscript.

Since the data processing part is not the most important part of this manuscript, we have not added all the description to the revised manuscript.

Changes:

We have updated the description of data processing in Line 64-71.

Other comments :

- Abstract (L. 7) : 12 May 2012 → 12 May 2008.

We have modified.

- Introduction : L. 22-27 is confusing as it gives the impression that precursory strain has been detected prior to the 2013 Ruisui earthquake (Canitano et al., 2015), which has not.

Besides, as the study involves the use of strain signals to study preseismic changes, it would be interesting to have exemples of previous studies which aimed to detect changes in the hypocentral regions of large earthquakes using strain data. For instance, short- period strain observations prior to the 1987 Supersition Hills earthquake (Agnew & Wyatt, 1989), 1989 Loma Prieta EQ (Johnston et al., 1990), 2010 L'Aquila (Amoruso & Crescentini, 2010) or 2013 Ruisui (Canitano et al., 2015) were all unsuccesfull. Note that those studies have been conducted on several stations located in the near-field of the shock, therefore under more optimal detection conditions.

Response:

Thank you for your suggestion. Canitano also gave us a short comment about his research. We have updated our expression.

Besides, we have supplemented these references in "Introduction".

- L. 25: 'borehole strain data, which record the direct crustal changes' →borehole strainmeters which detect the crustal changes. Why 'direct' crustal changes ?

Response:

Earthquake occurrence is the process of mechanics. "Direct" indicates that the borehole strain also record force, to distinguish from other kinds of observations. Strictly speaking, "direct" is a little inaccurate.

Changes:

We have modified as "Borehole strainmeters which detect the crustal changes"

- L. 43 : non-Gaussian → non-Gaussian distribution

We have modified.

- L. 57-58 : Â´ n Hence, it is implied ... preparation processes Â˙ z : do you have a reference for this sentence ?

Response:

This is our language expression problem. In fact, this sentence follows the last two paragraphs. There are 3 references among them indicate this point of view, then, there are 2 other references in this paragraph also support this sentence.

Changes:

We have modified this sentence into in Line 36. "Thereby, it is possible that precursor

anomalies lead to an increase of disordered components in observation data."

-L. 65-66 : 'dozens of meters' : can you be more specific ?
Yes, we have been more specific.
"… have been deployed at depths of more than 40 metres …"

- L. 178-180 : it is not clear why negentropy anomalies clustered on the left side of the parabola could be a signature of crustal deformation related to earthquake ?

Response:

There are two main reasons. First of all, these anomalies are different from this normal background. Since after the data processing, it is normal for the daily strain to be Gaussian distribution. Secondly, since the similar characteristics of the anomalies cause the cluster phenomenon to appear on the parabola before and after the Wenchuan earthquake.

Whether the negentropy falls on the left or right side of the parabola is determined by the sign of the skewness. The relationship between skewness and data distribution is as shown in Fig. 10. Negentropy anomalies (red points in Fig. 6 in the manuscript) clustered on the left side of the parabola shows that the observations of these abnormal days have negative skewness. In other words, there are a lot of negative extreme values in the observations of these days.

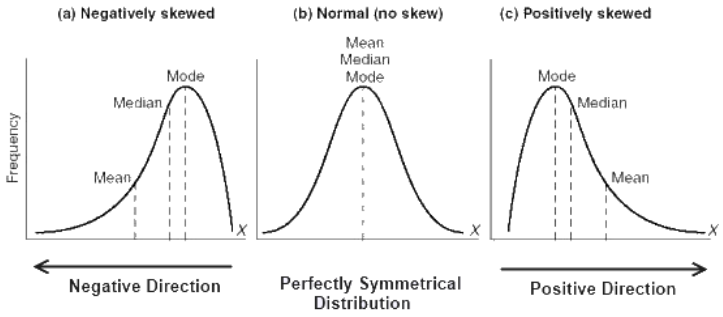

Fig. 10. Schematic diagram of the relationship between skewness and data distribution. Source: https://ss.csdn.net/p?https://mmbiz.qpic.cn/mmbiz_png/heS6wRSHVMkoXmWbecSLSvBtFqZRJW9MPickoP99bO1zu6cbtBuI34xjKpOObcRGErLkeSVGRrToJgd8Cria3tqw/640?wx_fmt=png.

From Fig. 6 (b) in the manuscript, we can see as the earthquake approaches, the abnormal days are basically clustered on the left side of the parabola. According to W. Marzocchi et al. (2014), spatio-temporal clustering is generally believed to represent the most striking departure from randomness for the large earthquake occurrence process.

Therefore, we suspect negentropy anomalies clustered on the left side of the parabola could be related to the earthquake. In order to study the possible correspondence with the earthquake process, we calculate the cumulative frequency of negentropy anomalies later in the manuscript.

Changes:

We have updated this sentence as “Besides, the extracted negentropy anomalies are clustered strongly on the left side of the parabola, which exhibit similar characteristics different from the normal Gaussian distribution.”

- L. 200: please consider remove ’famous’.
We have removed “famous”.

- L. 237-238: the authors stated that anomalies increased in 2008 when earthquake approaches and decreased after. That’s no so obvious according to Fig. 4 for which anomaly rate seems to increase after the earthquake. Can you explain why?

Response:

The anomalies there refer to the frequency of anomalies. In fact, the anomalies did not decrease immediately after the earthquake, since the earth's crust was still in a very unstable stage. As of October 2008, there are more than 900 aftershocks (Ms>3.0) as shown in the Fig. 1.

However, after extracting the negentropy anomalies that greater than the threshold in Fig. 4 in the manuscript, we calculated the cumulative frequency of negentropy anomalies and fit them by sigmoid function as shown in Fig. 8 in the manuscript. Based on the fitting result for the entire process in Fig. 8, we see the inflection point is almost at the earthquake moment. And before the inflection point, the accumulation of anomaly frequency has an exponential increase trend. After the inflection point, there is an opposite increase trend. Therefore, we stated that anomalies increased when earthquake approaches and decreased after.

- L. 244-245: Can you explain how you link the earthquake moment with the estimate of the inflection point based on negentropy analysis? What does that mean that the earthquake moment is proved to be a critical time during the earthquake?
- Fig. 8: where is the critical point? Can you explain it further?

Response:

We calculated the cumulative frequency of negentropy anomalies. Since in general, accumulated value of a typical random process usually has a linear increase. In particular, in case of critical phenomena, we would expect more frequent anomalies when they approach the critical point, and less frequent anomalies after (De Santis, A. et al. ,2017). However, the cumulative frequency of negentropy anomalies is well fitted by sigmoid function.

Sigmoid function is expressed as

$$y = A2 + \frac{(A1 - A2)}{(1 + e^{\frac{x - x0}{dx}})},$$

where $A1$, $A2$, $x0$ and dx are calculated by fitting and $x0$ is the inflection point of the function. The sigmoid function is a power law temporal behavior with an upper concavity and a subsequent power-law behavior after the inflection, with an opposite

concavity.

Also, the value of $x0$ obtained in the fitting result is very close to the time of the Wenchuan earthquake as shown in the Fig. 8 in the manuscript. The inflection point is the black vertical solid line, the earthquake day is the black dashed line. The two lines almost coincide in the Fig. 8 in the manuscript.

Therefore, we link the earthquake moment with the estimate of the inflection point.

Since the fitting curve is concave upward before the earthquake and concave downward after the earthquake. As the earthquake approaches, the slope of the curve increases, reaching its maximum near the earthquake, and then slowly decreasing.

Therefore, we stated the earthquake moment is proved to be a critical time during the earthquake. We also learned from De Santis, A. et al. (2017), they calculated the cumulative number of magnetic anomalies detected by Swarm satellite and also fit it by the sigmoid function. They thought inflection point in this function is a reasonable estimation of the time of the significant change in the critical dynamical system.

In Fig. 8, the critical point refers to the inflection point. We have unified the words as “infection point” and supplemented a brief explanation in Line 169-171 and Line 177-181.

Reference:

Su K. Z., Earthquake-monitoring capability of borehole strainmeter Earthqauke, vol (5): P38-46, 1991.

Qiu Z H, Tang L, Zhang B H, et a1 . Extracting anomaly of the Wenchuan Earthquake from the dilatometer recording at NSH by means of Wavelet-Overrun Rate Analysis . Chinese J . Geophys. (in Chinese), 2012, 55(2): 538-546, 2012.

De Santis, A., et al. Potential earthquake precursory pattern from space: The 2015 Nepal event as seen by magnetic Swarm satellites. Earth and Planetary Science Letters 461: 119-126, 2017.

W. Marzocchi, D. Melini. On the earthquake predictability of fault interaction models. Geophysical Research Letters, 41(23): 8294-8300, 2014.

Amoruso, A. and L. Crecentini. Limits on earthquake nucleation and other pre-seismic phenomena from continuous strain in the near field of the 2009 L’Aquila earthquake. Geophysical Research Letters, 37(10), L10307, 2010

Johnston M. J. S., Linde A. T., Gladwin M. T., Near-field high resolution strain measurements prior to the October 18, 1989, Loma Prieta Ms 7.1 earthquake. Geophysical Research Letters, 17(10): 1777-1780, 1990.

Agnew D. C., Wyatt F. K. The 1987 Superstition Hills earthquake sequence: Strains and tilts at pinon flat observatory. Bulletin of the Seismological Society of America, 79(2): 480-492, 1989

Kong, X., et al. A Detection Method of Earthquake Precursory Anomalies Using the Four-Component Borehole Strainmeter. Open Journal of Earthquake Research 07(02): 124-140, 2018.

Sun X L, Wang, G C, Yan R. Extracting high-frequency anomaly information fluid

observational data: a case study of the Wenchuan Ms8.0 earthquake of 2008. Chinese J. Geophysics. (in Chinese), 59(5):1673-1684, 2016.
Yan R., et al. Study on critical slowing down phenomenon of radon concentrations on water before the Wenchuan earthquake Ms8.0 earthquake. Chinese J. Geophysics. (in Chinese), 54(7):1817-1826, 2011.

We tried our best to improve the manuscript and made some revisions in the manuscript. These revisions will not influence the content and framework of the paper.

We appreciate for Editor and Reviewers' warm work earnestly, and hope that the correction will meet with approval.

Once again, thank you for your advice, hope to be able to learn more knowledge from you.

Appendix:

Kong X., et al. (2018) extracted the anomalies of the outgoing longwave radiation (OLR) data by calculating CD value (they defined).

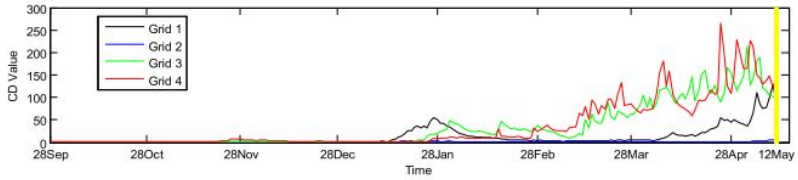

Fig. 8. Comparative CD value of grids 1, 2, 3, 4 in Wenchuan area, from 28th September, 2007 to 12th May , 2008, yellow line represents Wenchuan earthquake date.

Sun X. L., et al. (2016) extracted the anomalies of the fluid data by calculating λ^2.

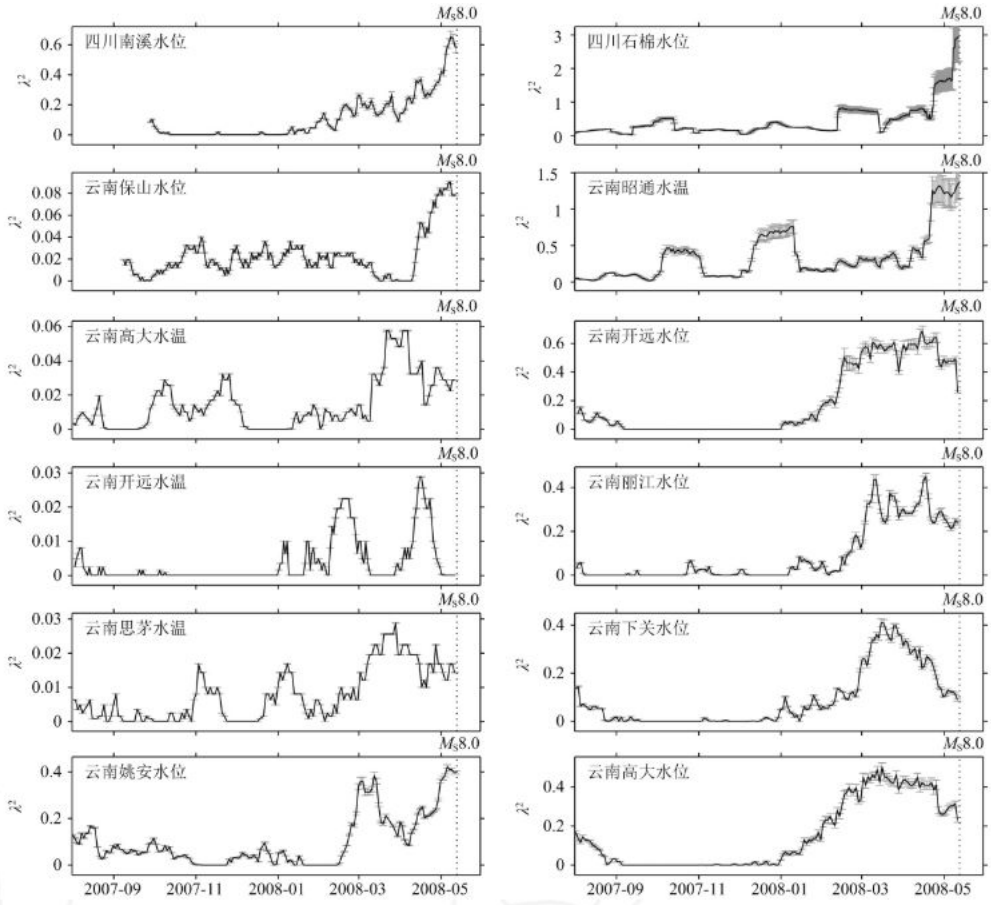

图 6 汶川 8.0 级地震前流体高频信息异常曲线

Fig. 6 Curves of high-frequency fluid anomaly information before Wenchuan M_S8.0 earthquake

Yan R., et al. (2011) extracted the anomalies of the radon concentrations by calculating AR(1) coefficient (they defined).

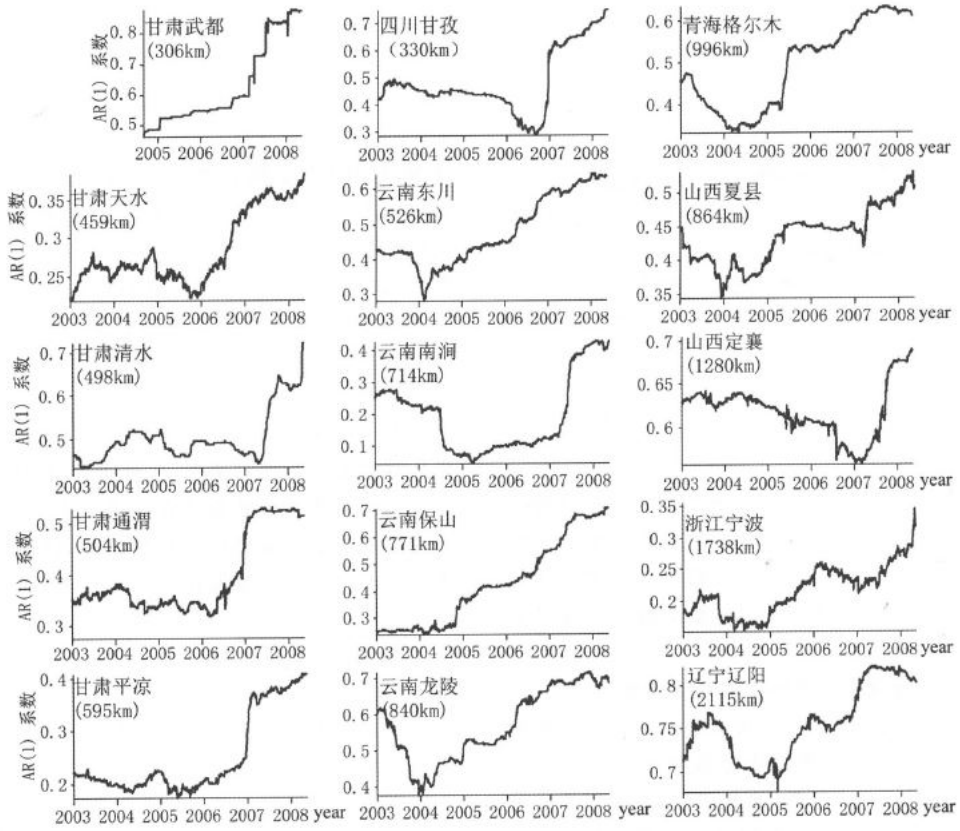

图 10　汶川 8.0 级地震前中国大陆水氡存在临界慢化现象的 AR(1)系数曲线
（括号中的数字表示距离汶川 8.0 级主震震中的距离）

Fig. 10　AR(1) coefficient curves of water radon for the existence of critical slowing down phenomenon before Wenchuan 8.0 earthquake in China mainland. (Numbers in parentheses denote the distance from epicenter of Wenchuan 8.0 main earthquake)

Negentropy anomaly analysis of the borehole strain associated with the Ms 8.0 Wenchuan earthquake

Kaiguang Zhu[1,2], Zining Yu[1,2], Chengquan Chi[1,2], Mengxuan Fan[1,2], and Kaiyan Li[1,2]

[1]College of Instrumentation and Electrical Engineering, Jilin University, China
[2]Key Laboratory of Geo-Exploration Instrumentation, Ministry of Education, Jilin University, China

Correspondence: Kaiguang Zhu (zhukaiguang@jlu.edu.cn)

Abstract. A large earthquake of 8.0 magnitude occurred on 12 May ~~2012~~2008, 14:28 UTC, with the epicenter in Wenchuan. To investigate the pre-earthquake anomalous strain changes, negentropy is introduced to borehole strain data at Guza station, approximated by skewness and kurtosis revealing the non-Gaussianity of recorded fluctuations. We separate the negentropy anomalies from the background by Otsu's method and accumulate the anomaly frequency in different scales. The results show the long-scale cumulative frequency of negentropy anomalies follows a sigmoid behaviour, while the inflection point of the fitting curve is close to the occurrence of the earthquake. For the short-scale analysis before the earthquake, there are two cumulative acceleration phases~~corresponding to the two crustal stress releases, indicating the preparation process of the Wenchuan earthquake. We consider that negentropy~~ . Combined with the confusion discussion for different time periods and stations, we consider the negentropy analysis exhibits potential for ~~the analysis of earthquake precursor~~ studying pre-earthquake anomalies.

1 Introduction

Changes in crustal deformation fields over time have ~~preceded~~ been recorded at least some large earthquakes (Thatcher, W. et al., 1981), such as the 2011 Tohoku earthquake (Hitoshi Hirose, 2011) and the Ruisui earthquake in Taiwan in 2013 (Canitano A. et al., 2015) . Borehole ~~strain data, which record the direct crustal changes ,~~ strainmeters which detect the crustal changes provide an opportunity to investigate preparation process prior to earthquakes~~(Linde~~ . Many strain observations were of research significance (Linde A. T., et al.,1996, Hsu, Y. ~~-J~~J. et al., 2015)~~.~~, although there were some unsuccessful detections, such as 1987 Superstition Hills earthquake (Agnew D. C., et al., 1989), 1989 Loma Prieta earthquake (Johnston et al., 1990) and 2009 L'Aquila earthquake (Amoruso A., et al., 2010).

Various methods are used in identifying borehole strain anomalies based on large amount of monitoring data. Experienced scholars extract borehole strain anomalies by discriminating patterns of waveform behaviors compared to those during the normal stage (Johnston M.J.S. ~~Johnston~~ et al., 2006, Chi S. L. et al., 2014). In the time domain, Qiu Z. H. et al. (2010) identified abnormal strain changes by overrun rate and wavelet decomposition for the Wenchuan earthquake. While in the frequency domain, Qi L. et al. (2011) thought the signal with a period of 10 to 60 minutes might be anomalies through S-transform compared with the background signal. In addition, statistical methods are proved effective in distinguishing borehole

strain anomalies with regard to large earthquakes, such as principal component analysis (Zhu K. G. et al., 2018) and correlation coefficients along with the consistency relation (Kong X. et al., 2018).

The probability distribution function (PDF) of observation data is also an informative way of extracting potential anomalies contained in earthquake generation processes. P. Manshour et al. (2009) extracted variance anomalies of the probability density of the Earth's vertical velocity increments, and successfully found a pronounced transition from Gaussian to non-Gaussian distribution prior to 12 moderate and large earthquakes. Before the Wenchuan earthquake, the high-frequency fluid observational data deviated from Gaussian distributions at 16 water level and 14 water temperature stations (Sun X. L. et al., 2016).

Rather than the whole PDF, often its moments are utilized, moments may be estimated quite reliably from relatively small amounts of data (Sattin, F. et al., 2009). In 2016, Chen H. J. et al. applied skewness and kurtosis (the third- and fourth-order moments) of the geoelectric data to pick up non-Gaussian distribution anomalies to predict impending large earthquakes in Taiwan. On the other hand, for turbulent or disordered systems, the non-Gaussian distribution of time series in skewness-kurtosis domain attracts attention. Observation data series from various fields of geophysics indicate that a parabolic relation between skewness and kurtosis holds in fields such as seismology (M. Cristelli, et al., 2012), oceanography (Sura, P. et al., 2008) and atmospheric science (A. Maurizi, 2006).

~~Hence~~Thereby, it is ~~implied that possible precursor anomalies deviate from Gaussian distribution during earthquake preparation processes.~~ possible that precursor anomalies lead to an increase of disordered components in observation data. K. Eftaxias et al. (2008) proved that the pre-catastrophic stage could break the persistency and high organization of the electromagetic field through studying fractional-Brownian-motion-type model using laboratory and field experimental electromagetic data. In view of Lévy flight and Gaussian processes, Lévy flight mechanism prevents the organization of the critical state to be completed before earthquakes, since the long scales are cut-off due to the Gaussian mechanism (S.M. Potirakis et al., 2019).

Entropy can serve as a measure of the unknown external energy flow into the seismic system (Akopian, S. T., 2015). K. Karamanos et al. (2006, 2005) quantified and visualized temporal changes of the complexity by approximate entropy, they claimed significant complexity decrease and accession at the tail of the preseismic electromagnetic emission could be diagnostic tools for the impending earthquake. Ohsawa Yukio (2018) detected earthquake activation precursors by studying the regional seismic information entropy on earthquake catalog.

Negentropy definition is based on the entropy and it is also widely used to detect non-Gaussian features. Li Y., et al. (2018) proposed an arrival-time picking method based on negentropy for microseismic data. In this study, the negentropy is applied to borehole strain at Guza station associated with the Wenchuan earthquake, approximated by skewness and kurtosis revealing the non-Gaussianity of borehole fluctuations. Subsequently we study the extracted negentropy anomalies in different scales to investigate correlations with crustal deformation. Furthermore, we did a confusion discussion for different time periods and stations.

2 Observation

YRY-4 borehole strainmeters, which are designed to record continuous deformation occurring over periods of minutes to years, have been deployed at depths of ~~dozens of~~ more than 40 metres at more than 40 terrain-sensitive locations within China. These strainmeters are capable of resolving strain changes of less than one-billionth. The data sampling rate is once per minute.

The study period is from January 1, 2007, to June 30, 2009. The ~~object of the study is the Wenchuan Ms 8.0 earthquake in the region, which is shown in Figure.~~ study area is shown in Figure. 1. We find the Guza station stands on the southwestern end of the Longmenshan fault zone. Besides, the epicentre is about 150km away from the station, which is within the monitoring capability of the borehole strainmeters (Su. K. Z., et al., 1990).

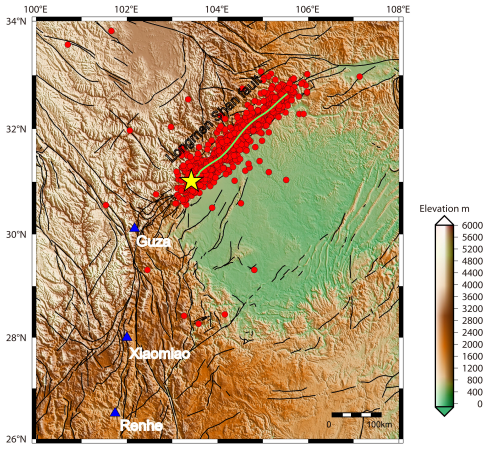

Figure 1. Location map showing the epicentre ~~of the Wenchuan earthquake epicentre~~ and ~~the Guza station~~three stations. The ~~Wenchuan earthquake occurred at 14:28:04 on May 12, 2008 (UTC+8). The magnitude of the earthquake was Ms 8.0, and the focal depth was approximately 14 km. The~~ epicentre was located ~~in Wenchuan County, Sichuan Province,~~ at 31.01°N, 103.42°E. The red circles are aftershock distribution from the main shock to October 2008. The green curve is the schematic curve of the main rupture zone and black curves are faults.

Because the four gauges of the YRY-4 borehole strainmeter are arranged at 45° intervals, this design has improved its self-consistency. This arrangement produces four observation values: S_i, $(i = 1, 2, 3, 4)$ (Qiu Z. H.,et al., 2013). The self-consistency as shown in equation (1), which can be used to test the reliability of the data among the four gauges.

$$S_1 + S_3 = S_2 + S_4 \tag{1}$$

In practical application, the higher the correlation between both sides of the equation (1), the more reliable the data. ~~Generally, we use~~ In that case, we can use areal strain S_a ~~for the areal strain in~~ for describing the subsurface strain state ~~of the observation area as shown in equation 2.~~ instead of four component observations. S_a is expressed as

$$S_a = (S_1 + S_2 + S_3 + S_4)/2. \tag{2}$$

The borehole strain of Guza station is highly consistent ~~among the four gauges at the Guza station (Qiu~~ (Qiu Z. H., et al., 2009) ~~,~~ as shown in Figure. 2.

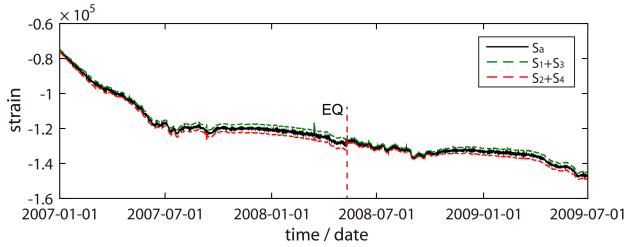

Figure 2. Self-consistency of the borehole strain at Guza from January 1, 2007, to June 30, 2009.

We first calculate the ~~difference in the data because in the borehole strain data, the change in the strain is a concern (Li Jinwu et al. , 2014).~~ differential signals to remove the low frequency information, including borehole trend, low frequency effects of the air pressure and temperature on the signals. We then remove the ~~components associated with the solid tide frequencies~~ periodic terms of the signals through a daily harmonic analysis. The ~~remaining~~ residual high-frequency signals are shown in Figure. 3. In particular, small changes in the curve are amplified by the processing.

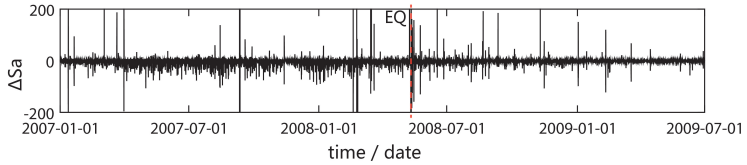

Figure 3. High-frequency areal strain at Guza from January 1, 2007 to June 30, 2009.

3 Methodology

3.1 Negentropy and non-Gaussianity

The entropy-based negentropy is a statistically justified measure of non-Gaussianity (A. Hyvarinen, et al., 2000). The entropy of a random variable $X = \{x_1, x_2, ..., x_i, ...\}$is defined as

$$H(X) = -\sum_i P(X = x_i) \log P(X = x_i), \tag{3}$$

where P is the probability density function. Entropy measures the randomness of a random variable. The Gaussian random variable has the largest entropy of all other random variables with equal variance (T.M. Cover et al., 1991). The definition of negentropy is given by

$$J(X) = H(X_{guass}) - H(X), \tag{4}$$

in which X_{gauss} is a Gaussian random variable with the same mean and covariance matrix as X. The entropy of a Gaussian random variable can be estimated by

$$X_{guass} = \frac{1}{2}\log|\det\Sigma| + \frac{n}{2}(1+\log 2\pi), \tag{5}$$

where n is the dimension of the variable, and Σ is its covariance matrix.

However, the theoretical calculation of negentropy also depends on the prior probability density of random variables and other information which are difficult to determine accurately. In practical applications, higher order statistics (HOS) and density polynomial expansion are usually used to approximate one-dimensional negentropy (Jones, M. C. et al., 1987). The approximation results are as follows:

$$J(X) \approx \frac{1}{12}skewness^2(X) + \frac{1}{48}kurtosis^2(X). \tag{6}$$

This definition suggests that any deviation from a Gaussian distribution will increase the negentropy $J(x)$. The skewness and kurtosis are the third- and fourth-order statistics, respectively, which are defined as

$$skewness(X) = \frac{\mu_3}{\sigma^3} = \frac{E[(X-\mu)^3]}{E[(X-\mu)^2]^{3/2}} \tag{7}$$

and

$$kurtosis(X) = \frac{\mu_4}{\sigma^4} = \frac{E[(X-\mu)^4]}{E[(X-\mu)^2]^2} - 3, \tag{8}$$

where μ is the mean of X and σ is the standard deviation of X. Skewness is a measure of asymmetry in a PDF. A symmetric distribution has zero skewness. Kurtosis is a measure of the heaviness of the tails. Distributions that are more outlier-prone than the normal distribution have kurtosis values greater than zero.

Moreover, the relation between the skewness and kurtosis is universal, they approximately align along a quadratic curve (Sattin, F., et al., 2009):

$$kurtosis(X) = A \cdot skewness^2(X) + B. \tag{9}$$

Here we calculate the normalized skewness and kurtosis in the study period, so equation (9) can be derived into

$$kurtosis(X) = A \cdot (skewness^2(X) - 1), \tag{10}$$

indicating the test day is super-Gaussian when the skewness is outside the range (-1,1).

This relation is trivial in a Gaussian fluctuating system; it reduces to a fixed mass around zero (skewness=0 and kurtosis=0). In a turbulent environment where fluctuating quantities obey non-Gaussian statistics, the moments obey the above relation.

3.2 Otsu's thresholding method

To solve the negentropy anomaly detection problem, we designed a simple thresholding hypothesis test using the Otsu method (Otsu, 1979) that provides an optimal separation between background and seismic-related activities. For any given value k, we can separate the previously calculated $J(x)$, as shown in equation (6), into the following two classes:

$$\begin{aligned} C_0(k) &= \{J(x) \leq k\}, \\ C_1(k) &= \{J(x) > k\}. \end{aligned} \tag{11}$$

Using these classes, the weighted average value $\mu_T(x)$ of $J(x)$ can be expressed as follows:

$$\begin{aligned} &\mu_T(x) = \lambda_0(k)\mu_0(x;k) + \lambda_1(k)\mu_1(x;k), \\ &\lambda_0(k) + \lambda_1(k) = 1. \end{aligned} \tag{12}$$

where $\mu_0(x;k)$, $\mu_1(x;k)$ are the mean values of the class $C_i(k)$, i=0, 1, and $\lambda_i(k)$ is the percentage of points belonging into each class. Following the thresholding scheme of Otsu (1979), we define the following cost function:

$$\begin{aligned} {\sigma_B}^2 &= \lambda_0(k)(\mu_0(x;k) - \mu_T(x;k))^2 + \lambda_1(k)(\mu_1(x;k) - \mu_T(x;k))^2, \\ &= \lambda_0(k)\lambda_1(k)(\mu_1(x;k) - \mu_0(x;k))^2. \end{aligned} \tag{13}$$

where ${\sigma_B}^2$ is the within-class variance of negentropy. Then, by finding the k^* value searching for k when ${\sigma_B}^2$ becomes the maximum

$$k^* = \arg\max_k {\sigma_B}^2(k), \tag{14}$$

the optimal value k^* here separates the background set and anomaly set.

In this test, our initial assumption is that the sliding window is composed of a Gaussian signal of non-seismic-related activities. When our test negentropy exceeds the critical value k*, this initial hypothesis is not valid, and the alternative is true, indicating the presence of a negentropy anomaly within the window.

4 Results

According to the empirical hypothesis that geophysical signals deviate from the Gaussian distribution when they record abnormal activities, and based on the results of previous studies, we perform the following investigation.

4.1 Extracting negentropy anomalies

As the negentropy is calculated using a 2-hour long sliding window, we assume that it reaches the maximum values when the time window contains anomalies from seismic-related activities. The negentropy during the study period is shown in Figure. 4.

The within-class variance ${\sigma_B}^2$ and negentropy value distribution are compared in Figure. 5. According to equations (11) to (14), when $k^* = 1.1130$, ${\sigma_B}^2$ reaches its maximum. Therefore, the negentropy were separated by k^* into the quasi-Gaussian

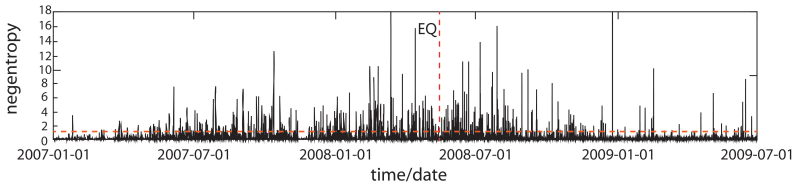

Figure 4. Negentropy at Guza from January 1, 2007, to June 30, 2009. The red dotted, horizontal line is the optimal threshold k^* calculated by Otsu method.

background and non-Gaussian anomalies from 2007 to 2009. Otsu threshold k^* here is consistent with the accuracy of the negentropy and the strain data. The YRY-4 borehole strainmeter has a measurement accuracy of 10^{-9}, however, we usually cutoff four digits after the decimal point in practical calculations.

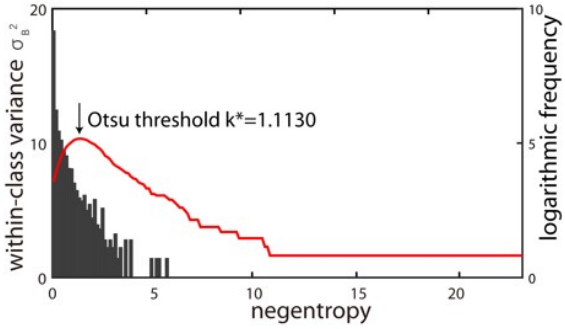

Figure 5. Within-class variance ${\sigma_B}^2$ of the negentropy (red line) and negentropy histogram.

In the skewness-kurtosis domain, the statistical relationship of the borehole areal strain is consistent with parabolic behaviour as described in equation (10) (Figure. 6(a)), verifying that the turbulent system of borehole strain is significantly non-Gaussian. ~~However~~Besides, the extracted negentropy anomalies are clustered strongly on the left side of the parabola, which ~~could be a signature of crustal deformation related to the earthquake~~exhibit similar characteristics different from the normal Gaussian distribution. Here, there are four points on the right side; one occurred in early 2007, and the others occurred after the earthquake. Therefore, we will not discuss them in the following.

In addition, as shown in Figure. 6(b), at times far from the earthquake, the negentropy distribution is basically Gaussian in the skewness-kurtosis domain. However, at times closer to the earthquake, the relatively stable state was broken due to the non-Gaussian mechanism, with more negentropy anomalies appearing on the left side of the parabola. While in 2008, almost all of the negentropy present left-skewed.

~~These~~ The phenomena prompt us to study ~~the origin of this left-skewed distribution and~~ its possible correspondence with the seismogenic process.

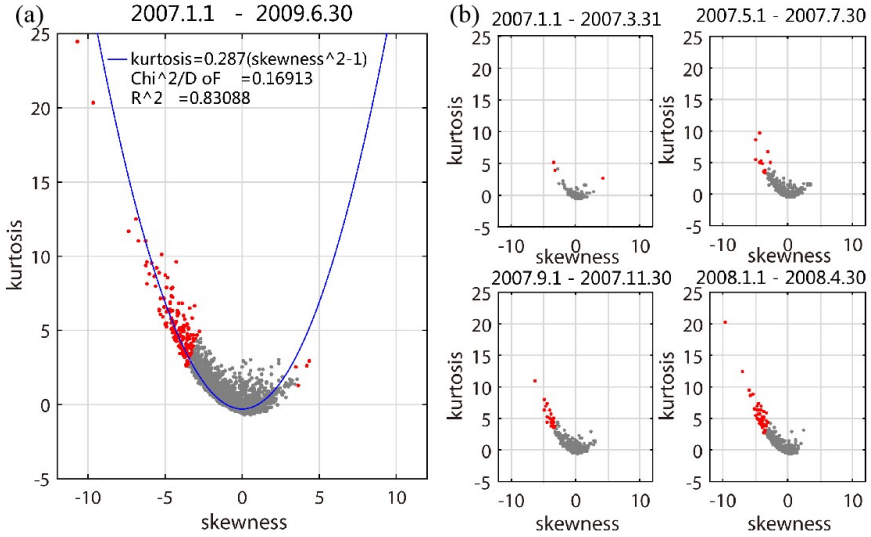

Figure 6. Negentropy distributions in the skewness-kurtosis domain in (a) January 1 ,2007, to June 30 2009, and (b) four shorter periods before the earthquake. Red denotes that the negentropy is greater than k^*, and grey indicates that the negentropy less than k^*. The blue curve is the quadratic fit with a 95% confidence.

4.2 Negentropy anomaly frequency accumulation

The transition of negentropy anomalies in the skewness-kurtosis domain is quantified as the change of the anomaly frequency per unit time through a logarithmic-linear model. Logarithmic-linear models are often used of interest to estimate the expected frequency of the response variable at the original scale for a new set of covariate values, such as the ~~famous~~ Gutenberg-Richer law, in which a linear relationship exists between the logarithm of the cumulative number of seismic events of magnitude M or greater versus the magnitude M (Gutenberg and Richer, 1954).

The logarithmic-linear regression model is proposed as

$$\log N = \beta_1 \times k_J + \beta_0 + \varepsilon, \tag{15}$$

where k_J takes different threshold values according to the $J(x)$ values, N is the number of occurrences in which J is greater than or equal to threshold k_J, β_1 and β_0 are the regression coefficients, where a lower slope β_1 indicates that there are more higher J values, implying there are more anomalies at that moment, and ε is the random error that represents the model uncertainty.

We use the logarithmic-linear model to solve the relationship between the negentropy anomaly frequency and different thresholds each day using the ordinary least squares method (OLS) method. Afterwards, an optimal threshold k^*, calculated by the Otsu method, is chosen for all models, where

$$N_J(t) = \exp(\beta_1(t) \times k^* + \beta_0(t) + \varepsilon(t)) \tag{16}$$

and the $N_J(t)$ under the threshold k^* is shown in Figure. 7. The model theoretically solves the problem of selecting the length of the time window. In addition, the estimated $N_J(t)$ is considered as the expected frequency of anomalies.

The goodness of fit for each logarithmic-linear model was evaluated using analysis of

$$R^2 = 1 - \sum_{i=1}^{n}(N_i - \hat{N}_i)^2 / \sum_{i=1}^{n}(N_i - \overline{N_i})^2 \tag{17}$$

and the root-mean-squared error(RMSE).

$$RMSE = \sqrt{\sum_{i=1}^{n}(N_i - \hat{N}_i)^2 / n}. \tag{18}$$

The R^2 and RMSE values in the study period (912 days) show that the logarithmic-linear relationship can explain the relationship between the negentropy anomaly frequency and different thresholds. The mean of R^2 is 0.9695, which is close to 1, and the variance of R^2 is 0.0435. The mean and variance of the RMSE are also small (0.1098 and 0.1301, respectively).

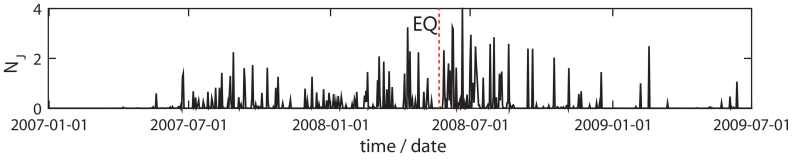

Figure 7. Estimated expected frequency N_J under the optimal threshold k^*

~~In general, accumulated value of a typical random process usually has an linear increase. The~~ We calculate the negentropy cumulative frequency of the study period ~~is~~ as shown in Figure. 8. ~~We not only do~~ There is not only a long-scale analysis of the whole ~~earthquake process~~period, but also ~~carry out~~ a short-scale analysis of the pre-earthquake process. In general, accumulated value of a typical random process usually has a linear increase. In particular, in case of critical phenomena, we would expect more frequent anomalies when they approach the critical point, and less frequent anomalies after (De Santis, A. et al. ,2017).

For the entire earthquake process, a two-month long sliding window is selected for accumulation~~as shown in Fig.~~ . In Figure. 8(a)~~. Beginning in~~ , after July 2007, the negentropy anomalies gradually accumulated. Qiu (2009) and Chi (2014) also observed anomalies of this period at Guza station, they speculated that abnormal strain may reflect small-scale rock formation rupture before the earthquake. In particular, we find more frequent negentropy anomalies in 2008 as the earthquake approaches, and less frequent anomalies after, so a sigmoid function is used to fit the acceleration, before the earthquake and the deceleration after. ~~According to De Santis, A. et al. (2017),~~ Sigmoid function is expressed as

$$y = A2 + \frac{(A1 - A2)}{(1 + e^{\frac{x - x_0}{dx}})}, \tag{19}$$

where $A1$, $A2$, $x0$ and dx is the inflection point. The sigmoid function is a power-law temporal behavior with an upper concavity and a subsequent power-law behavior after the inflection point, with an opposite concavity. The inflection point in this function is a reasonable estimation of the time of the significant change in the critical dynamical system ~~. Our calculation~~ ~~shows that the inflection point x0 of~~ (De Santis, A. et al. ,2017). Also, the value of x0 (8.3337) obtained in the fitting result is almost coincide with the Wenchuan earthquake day. The actual time of the ~~optimal fitting~~ earthquake is ~~8.3337, which is surprisingly close to the actual time~~ (8.3871 ~~) of the Wenchuan earthquake~~ after conversion. Thus, ~~the earthquake moment is proved to~~ we consider the Wenchuan earthquake day may be a critical time during the whole Wenchuan earthquake process.

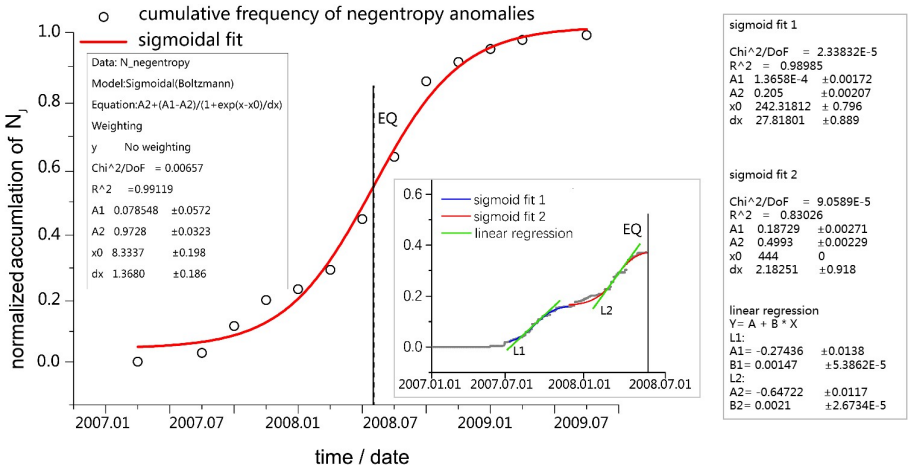

Figure 8. (a) Results of the long-scale negentropy anomaly frequency for the Wenchuan earthquake at Guza station from January 1, 2007, to June 30, 2009. Each circle represents an anomaly negentropy for 2 months. The cumulative frequency of negentropy anomaly is represented. The earthquake day is represented as a vertical ~~solid~~ black dashed line. The red line is a ~~sigmoidal~~ sigmoid fit that underlines ~~a critical~~ an inflection point (vertical ~~dashed~~ solid line) is close to the occurrence of the earthquake. (b) Results of the short-scale negentropy anomaly frequency prior to the earthquake, every grey point is an anomaly for one day, the blue and red lines are two segment sigmoid fit results. Two green lines represent the liner regression for the two phases, the first phase slope is 0.00147, the second one is 0.0021.

When we narrowed the accumulated window to one day, we observed two negentropy anomalies before the earthquake as shown in ~~Fig~~Figure. 8(b). The first anomaly frequency increase occurred from August to October 2007. In March 2008, there was a second phase of anomaly increase, and the cumulative frequency then slowly increased to a plateau period near the time of the earthquake. This probably due to the stress is in deadlocked phase. Since before the Wenchuan earthquake, the elastic deformation of the crust reaches its limit and the deformation is resisted in the hypocentral region, which is measured by GPS data (Jiang Z. S. , 2009).

These two phases prior to the earthquake are also approximated with sigmoid functions. In order to further compare the anomalies of the two phases, we use linear regression to fit the central part of the two sigmoid curves. We find that the second acceleration is greater than the first acceleration.~~We think the accumulations of these two negentropy anomalies may be an indication of crustal activity before the Wenchuan earthquake.~~

5 ~~Discussion and Conclusion~~

~~Previous studies for the Wenchuan earthquake are consistent with our findings. Wang (2018) concluded that an apparent stress change occurred after June 2007 based on multiple focal mechanisms. Likewise, we did not find negentropy anomalies in the first six months of 2007. In the large-scale analysis, we show that the cumulative frequency of negentropy anomalies follows the a power-law behaviour approaching a critical time that is close to the earthquake time, and then recovers as a typical recovery phase after the earthquake This process is consistent with the empirical phenomena before and after earthquakes, which is also similar with a potential earthquake precursory pattern in magnetic data from Swarm satellites by A. De Santis (2017) for the 2015 Nepal event. Qiu (2009) and Chi (2014) speculated that the areal strain indicates that the integrity of the medium around the borehole at the Guza station began to change significantly after August 2007, because the continuity of the medium in the source region of the Wenchuan earthquake was gradually deformed during the nucleation process. In our short-scale analysis, negentropy anomalies also present a acceleration in August 2007. The second acceleration in March 2008 is also consistent with the occurrence of a phase measured by GPS (Jiang Z. S., 2009), in which the elastic deformation of the crust reaches its limit, and the deformation is resisted in the seismogenic region before the earthquake. More importantly, we speculate that the two accelerations of the cumulative negentropy anomaly corresponding to two stress releases. Ma Jin (2014) proposed the deformation characteristics in the sub-instability stage of faults before earthquakes based on different experiments and several earthquakes.~~

Fault zones contain relatively weak and relatively strong parts. The former is the area where strain release begins, while the latter is the stress locking part and the beginning of rapid instability (Noda et al., 2013). Ma Jin (2014) proposed the deformation characteristics in the sub-instability stage of faults before earthquakes. She thinks accelerated expansion of the strain release zone in fault zone is a sign of entering the inevitable earthquake stage. There are two instabilities before earthquakes, the former is related to the release of weak parts, and the latter is related to the rapid release of strong parts ~~of the fault~~ during strong earthquakes. The accelerated expansion of the former promotes the occurrence of the latter. ~~We~~ Thus, we speculate that the two ~~negentropy anomaly accelerations may represent the two instabilities associated with the Wenchuan earthquake. The first corresponds to the start of strain release and the second larger one corresponds to the acceleration of instability, indicating that strong earthquakes are likely to occur. In our work, the extracted negentropy~~ accelerations of the cumulative negentropy anomaly may correspond to two stress releases.

5 Confusion discussion

5.1 Comparison of random time periods

We randomly selected the strain data for 200 days before and after March 20, 2011 and March 24, 2014 at Guza station. The selected data for the two periods are required to be in the absence of strong earthquakes and with higher quality. We performed negentropy analysis on these two observations and compared them with the results of negentropy analysis associate with the Wenchuan earthquake as shown in Figure. 9.

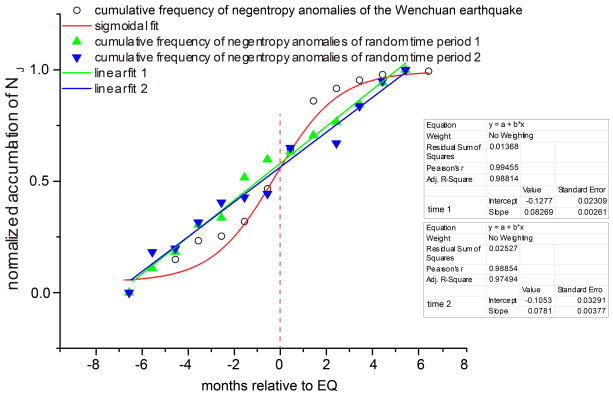

Figure 9. The comparative analysis of cumulative frequency of negentropy anomalies between earthquake period and random time periods. The zero point of green dots is March 20, 2011, the zero point of blue dots is March 24, 2014

As we can see in Figure. 9, The cumulative frequency of negentropy anomalies of random periods have linear increase. However, in the Wenchuan earthquake periods, as the earthquake approaches, the cumulative frequency of negentropy anomalies increases rapidly and recovered to a slow growth after the earthquake.

5.2 Comparison of different stations

We selected Xiaomiao station and Renhe station to find out if their observations received strain changes. Their locations are shown in Figure. 1. Compared with the Guza station, we did the negentropy analysis of these two stations as shown in Figure. 10.

As we can see in the Figure. 10, the cumulative frequency of negentropy anomalies of Xiaomiao station are also well fitted by the sigmoid function. The accumulation curve is growing rapidly before the earthquake and concave downward after which is similar to the Guza station, although the inflection point of Xiaomiao station is about two months preceding the earthquake moment. However, since the curve is approximately linear before and after the inflection point, the value of inflection point exists a range. Cumulative anomalies of the ~~short-period signal of borehole areal strain based on Otsu's thresholding associated with the Wenchuan earthquake~~ Renhe station are basically linear, indicating that the Renhe station may not receive pre-earthquake anomalies.

Renhe station is far from the end of the Wenchuan earthquake fault, so it is reasonable that no abnormal changes are observed. However, Xiaomiao station is located between the Guza station and Renhe station, and the fitting result shows that there is a similar trend to the Guza station, with a weaker curvature. So, for the nearest station to the epicentre, Guza station may able to receive more pre-earthquake anomalies.

Furthermore, Qiu (2012) found that the anomalies at Ningshan station were similar to the anomalies at Guza station. Such two stations have observed similar Wenchuan earthquake precursor anomalies, which may not be accidental. Since the

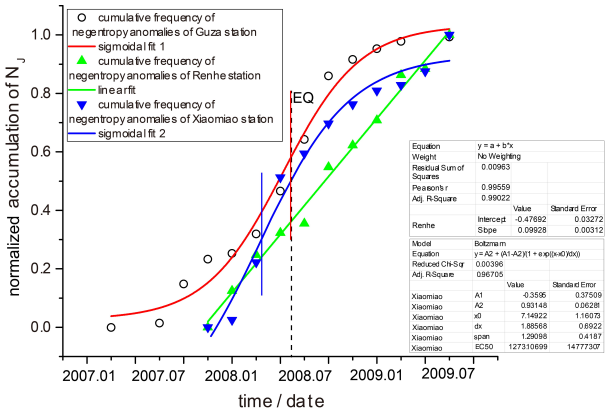

Figure 10. Cumulative frequency of negentropy anomalies of Xiaomiao station and Renhe station from September 16, 2007 to June 30, 2009. The negentropy analysis of Guza station is from January 1, 2007 to June 30, 2009, because of the different installation time of the instruments. The red vertical line is the inflection point of the fitting curve of Guza station. The blue vertical line is the inflection point of the fitting curve of Xiaomiao station. The black dotted line is the earthquake day.

Ningshan station is actually located at the northeastern end of the Longmenshan fault zone. This location is a correspondence with the southwestern end of the fault where the Guza station is.

5.3 Exclusion of meteorological factors

The strain signals are sensitive to a few meteorological factors, therefore, we display the pressure variations, temperature variations recorded at Guza station and the daily rainfall measured by Tropical Rainfall Measuring Mission (TRMM) satellite which are downloaded through the NASA GIOVANNI-4 for the same period and the same area (http://giovanni.gsfc.nasa.gov/giovanni/) in Figure. 11. There are clearly annual variations in the strain, air pressure, temperature and rainfall data. The air pressure and temperature have been steadily fluctuating within a certain range, and the rainfall is also shown to be more in summer and less in winter.

While we calculated the differential data of the strain for negentropy analysis. So, we make differential calculations for all three influencing factors as shown in Figure. 12.

We observed that the air pressure, temperature and rainfall didn't change abnormally during the period when the extracted anomalies increase, whether we do differential calculation. Therefore, we consider that the abnormal variations on the processed strain signals are not caused by these factors.

6 Conclusions

In our work, the extracted negentropy anomalies of borehole strain associated with the Wenchuan earthquake are analyzed. The cumulative frequency of negentropy anomalies are ~~analyzed.A logarithmic-linear model is proposed to estimate the~~

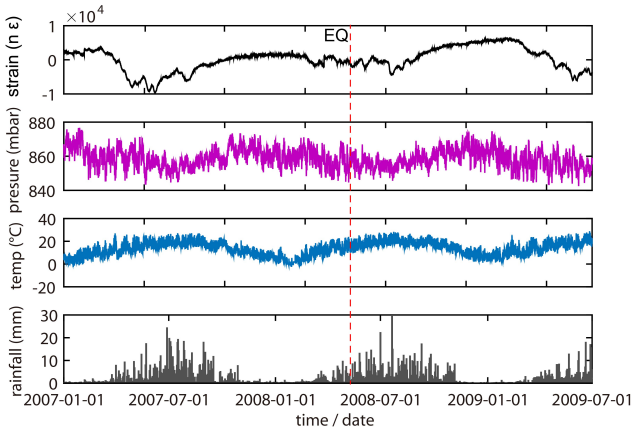

Figure 11. Borehole stain, air pressure, temperature and rainfall variations during study period at Guza station.

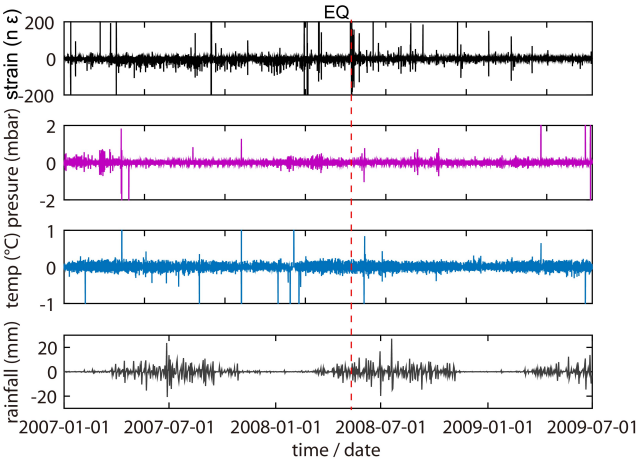

Figure 12. Differential borehole stain, air pressure, temperature and rainfall variations during study period at Guza station.

~~expected frequency of the left-skewed negentropy anomaly for everyday, and the evolution processes of the negentropy anomaly frequency are~~ studied in both long- and short-scale. Through the confusion discussion, we compare the cumulative anomalies of different time periods and different stations with those at Guza station during the study period~~. We consider~~, and preliminarily exclude meteorological factors. We suspect the negentropy anomalies ~~corresponding to crustal stress changes~~ at Guza station may have recorded abnormal changes related to the Wenchuan earthquake.

Since the tectonic dynamics of earthquakes during seismogenic and seismic processes are very complex, the mechanism of such abnormal changes is undoubtedly needed to be discussed. In particular, borehole strain signals are sensitive to external influence. Besides, because of the different characteristics and accuracy of different types of observations, a joint analysis has not been carried out yet. Further researches are needed to decipher a potential precursory phase. However, ~~which may be a~~

~~reflection of the subsurface medium and faults activities in the focal area associate with the Wenchuan earthquake. Moreover,~~ we may be able to ensure that the negentropy analysis has great potential in the study of earthquake precursors.

Data availability. The borehole strain data is a confidential information and therefore cannot be made publicly accessible. The air pressure and temperature data can be downloaded from National Earthquake Precursor Networks Center only through approval (qzweb.seis.ac.cn). The rainfall data are downloaded through the NASA GIOVANNI-4 (http://giovanni.gsfc.nasa.gov/giovanni/).

Author contributions. The authors contributed in accordance with their competence in the research subject. The first author Kaiguang Zhu was responsible for the key technical guidance and ideas. Zining Yu was responsible for method improvement, data analysis and manuscript preparation. Chengquan Chi helped to ensure the graph quality of the manuscript. Mengxuan Fan and Kaiyan Li contributed through active participation in the manuscript preparation.

Competing interests. The authors declare that they have no conflict of interest.

Acknowledgements. The authors ~~are appreciative of the Key Laboratory of the Geo-Exploration Instrumentation of Ministry of Education in Jilin University of China~~ would like to thank the China Earthquake Network Center providing the borehole strain data and NASA Giovanni team for rainfall data. Moreover, the authors are grateful to Professor ~~Zehua Qiu~~ Qiu Z. H. for his guidance and helpful suggestions. This research was supported by the Institute of Crustal Dynamics, China Earthquake Administration (Grant No.3R216N620537).

References

Agnew D. C., Wyatt F. K. The 1987 Superstition Hills earthquake sequence: Strains and tilts at pinon flat observatory. Bulletin of the Seismological Society of America, 79(2): 480-492,1989.

A. Hyvarinen, E. Oja. Independent component analysis: algorithms and applications, Neural Net. 13:411-430, 2000.

Akopian, S. T. Open dissipative seismic systems and ensembles of strong earthquakes: energy balance and entropy funnels. Geophysical Journal International 201(3): 1618-1641, 2015.

A. Maurizi. On the dependence of third- and fourth-order moments on stability in the turbulent boundary layer. Nonlinear Processes in Geophysics. 13(1):119-123, 2006.

Amoruso, A. and L. Crecentini. Limits on earthquake nucleation and other pre-seismic phenomena from continuous strain in the near field of the 2009 L'Aquila earthquake. Geophysical Research Letters, 37(10), L10307, 2010

Canitano, A., Hsu, YJ., Lee, HM. et al. Near-field strain observations of the October 2013 Ruisui, Taiwan, earthquake: source parameters and limits of very short-term strain detection, Earth, Planets and Space, 67(125), 2015.

Chen H.J., Chen C.C. Testing the correlations between anomalies of statistical indexes of the geoelectric system and earthquakes. Nat Hazards 84(2): 877-895, 2016.

Chi S.L., et al. Failure of self-consistent strain data before Wenchuan, Ludian and Kangding earthquake and its relation with earthquake nucleation. Recent Developments in World Seismology. 12:3-13, 2014.

De Santis, A., et al. "Potential earthquake precursory pattern from space: The 2015 Nepal event as seen by magnetic Swarm satellites. " Earth and Planetary Science Letters 461: 119-126, 2017. Gutenber

Gutenberg, B., Richer, C.F. Seismicity of the Earth and Associated Phenomena. Princeton University Press, Princeton, NJ, 1954.

Hirose, H. Tilt records prior to the 2011 off the Pacific coast of Tohoku Earthquake, Earth Planet and Space, 63(7): 665-658, 2011.

Hsu, Y. -JJ., et al. Revisiting borehole strain, typhoons, and slow earthquakes using quantitative estimates of precipitation-induced strain changes. Journal of Geophysical Research: Solid Earth, 120(6): 4556-4571, 2015.

Jiang Z. S, Fang Y., Wu Y.Q, et a1. The dynamic process of regional crustal movement and deformation before Wenchuan Ms8.0 earthquake. Chinese J. Geophys. (in Chinese), 52 (2):505-518, 2009.

Jones, M. C., and R. Sibson. What is projection pursuit?: Journal of the Royal Statistical Society Series A, 150, 1-37, 1987. Jiang Z. S

Johnston M. J. S., Linde A. T., Gladwin M. T., Near-field high resolution strain measurements prior to the October 18, Fang Y. 1989, Loma Prieta Ms 7.1 earthquake. Geophysical Research Letters, 17(10): 1777-1780, Wu Y.Q, et a1. The dynamic process of regional crustal movement and deformation before Wenchuan Ms8.0 earthquake . Chinese J. Geophys. (in Chinese), 52 1990.

Johnston M. J. S., Sasai Y., Egbert G. D., Mueller R. J. Seismomagnetic Effects from the Long-Awaited 28 September 2004 Ms6.0 Parkfield Earthquake. Bulletin of the Seismological Society of America, 96 (24B): 505-518, 2009. 206-220, 2006.

K. Eftaxias, Y. Contoyiannis, G. Balasis, K. Karamanos, J. Kopanas, G. Antonopoulos, G. Koulouras and C. Nomicos. Evidence of fractional-Brownian-motion-type asperity model for earthquake generation in candidate pre-seismic electromagnetic emissions. Nat. Haz. Earth Syst. Sci. 8, 657-669, 2008.

K. Karamanos, D. Dakopoulos, K. Aloupis, A. Peratzakis, L. Athanasopoulou, S. Nikolopoulos, P. Kapiris and K. Eftaxias. Study of pre-seismic electromagnetic signals in terms of complexity. Phys. Rev.E 74, 016104-016125, 2006.

K. Karamanos, A. Peratzakis, P. Kapiris, S. Nikolopoulos, J. Kopanas and K. Eftaxias. Extracting preseismic electromagnetic signatures in terms of symbolic dynamics. Nonlinear Processes in Geophysics 12, 835-848, 2005.

Kong, X., et al. A Detection Method of Earthquake Precursory Anomalies Using the Four-Component Borehole Strainmeter. Open Journal of Earthquake Research 07(02): 124-140, 2018.

Linde, A. T., M. T. Gladwin., M. J. S. Johnston., R. L. Gwyther and R. G. Bilham. A slow earthquake sequence on the San Andreas fault. J. Nature. 383. 65-68, 1996. ~~LiJ.W., Qiu Z. H. Analysis on strain tidal factor observed borehole strainmeters, Progress in Geophysics~~

Li, Y., ~~29(5): 2013-2018, 2014.~~ et al. Arrival-time picking method based on approximate negentropy for microseismic data. Journal of Applied Geophysics 152: 100-109, 2018.

Ma Jin, Guo Yan-shuang. Accelerated synergism prior to fault instability evidence from laboratory experiments and an earthquake case, Seismology and Geology, 36(3): 547-560, ~~2014~~ 2014.

M. Cristelli, A. Zaccaria and L. Pietronero. Universal relation between skewness and kurtosis in complex dynamics, Physical Review E, vol. 85(6):066-108, ~~2012 M. J. S. Johnston, Y. Sasai, G. D. Egbert, R. J. Mueller. Seismomagnetic Effects from the Long-Awaited 28 September 2004 Ms6.0 Parkfield Earthquake. Bulletin of the Seismological Society of America, 96 (4B): 206-220, 2006.~~ 2012.

Noda H, Nakatani M, Hori T. Large nucleation before large earthquakes is sometimes skipped due to ~~cascadeup Implications~~ cascade-up-Implications from a rate and state simulation of faults with hierarchical asperities. J Geophys Res Solid Earth, 118(6): 2924-2952, ~~2013~~ 2013.

Ohsawa, Y. Regional Seismic Information Entropy to Detect Earthquake Activation Precursors. Entropy 20(11), 2018.

Otsu, N. A threshold selection method from gray-level histograms: IEEE Transactions on Systems, Man and Cybernetics, 9:62-66, ~~1979~~ 1979.

P. Manshour, S. Saberi, Muhammad Sahimi, J. Peinke, Amalio F. Pacheco, and M. Reza Rahimi Tabar. Turbulencelike Behavior of Seismic Time Series.Phys. Rev. Lett. 102(1):014101, 2009.

Qi L., Jing Z. Application of S transform in analysis of strain changes before and after Wenchuan earthquake. J. Journal of Geodesy and Geodynamics. 4: 003, 2011.

Qiu Z. H., et al. Strain changes of four-component borehole strain network before the Wenchuan earthquake. Journal of Geodesy and Geodynamics, 29 (1): 1-5, 2009.

Qiu Z.H., Zhang B. H., Chi S. L., et al. Abnormal strain changes observed at Guza before the Wenchuan earthquake. J. Science China Earth Sciences. 54(2): 233-240, 2010.

Qiu Z. H., Tang L., Zhang B. H., et al. Extracting anomaly of the Wenchuan Earthquake from the dilatometer recording at NSH by means of Wavelet-Overrun Rate Analysis. Chinese J. Geophys. (in Chinese), 2012, 55(2): 538-546, 2012.

Qiu Z.H., Tang L., Zhang B., et al. In situ calibration of and algorithm for strain monitoring using four gauge borehole strainmeters (FGBS). J. Journal of Geophysical Research: Solid Earth. 118(4): 1609-1618, 2013.

Sattin, F., et al. About the parabolic relation existing between the skewness and the kurtosis in time series of experimental data. Physica Scripta, 79(4), 2009. ~~Sun XL~~

S.M. Potirakis, et al., Lévy and Gauss statistics in the preparation of an earthquake. Physica A: Statistical Mechanics and its Applications, 528, 121360, 2019.

Su K. Z., Earthquake-monitoring capability of borehole strainmeter Earthqauke, vol (5): P38-46, 1991.

Sun X. L., Wang, G C, Yan R. Extracting high-frequency anomaly information fluid observational data: a case study of the Wenchuan Ms8.0 earthquake of 2008. Chinese J. Geophysics. 59(5):1673-1684, 2016.

Sura, P. and P. D. Sardeshmukh. A Global View of Non-Gaussian SST Variability. Journal of Physical Oceanography 38(3): 639-647, 2008.

T.M. Cover, J.A. Thomas. Elements of Information Theory, Wiley, New York, 1991.

Thatcher, W., and T. Matsuda. Quaternary and geodetically measured crustal movements in the Tokai District, Central Honshu, Japan, J. Geophys. Res., 86(B10), 9237-9247, 1981. ~~Wang K Y, Guo Y S, Feng X. D. Sub-instability stress state prior to the 2008 Wenchuan earthquake from temporal and spatial stress evolution. Chinese J. Geophys. (in Chinese), 61(5): 1883-1890, 2018.~~

Zhu, Kaiguang, et al. Extracting borehole strain precursors associated with the Lushan earthquake through principal component analysis. Annals of Geophysics, 61(4):1593-5213, 2018.